RESEARCH ARTICLE

Highly Dynamic Cellular-Level Response of Symbiotic Coral to a Sudden Increase in Environmental Nitrogen

C. Kopp,[a]* M. Pernice,[b] I. Domart-Coulon,[c]* C. Djediat,[d] J. E. Spangenberg,[e] D. T. L. Alexander,[f] M. Hignette,[g] T. Meziane,[c] A. Meibom[b]

Laboratoire de Minéralogie et de Cosmochimie du Muséum, Muséum National d'Histoire Naturelle, Paris, France[a]; Laboratory for Biological Geochemistry, School of Architecture, Civil and Environmental Engineering (ENAC), École Polytechnique Fédérale de Lausanne (EPFL), Lausanne, Switzerland[b]; UMR BOREA-7208 MNHN/CNRS/IRD/UPMC, Muséum National d'Histoire Naturelle, Paris, France[c]; Plateforme de Microscopie Electronique, Muséum National d'Histoire Naturelle, Paris, France[d]; Institute of Earth Sciences, University of Lausanne, Lausanne, Switzerland[e]; Interdisciplinary Centre for Electron Microscopy (CIME), École Polytechnique Fédérale de Lausanne (EPFL), Lausanne, Switzerland[f]; Aquarium Tropical, Etablissement Public du Palais de la Porte Dorée, Paris, France[g]

* Present address: C. Kopp, Laboratory for Biological Geochemistry, School of Architecture, Civil and Environmental Engineering (ENAC), École Polytechnique Fédérale de Lausanne (EPFL), Lausanne, Switzerland; I. Domart-Coulon, UMR MCAM-7245 MNHN/CNRS, Muséum National d'Histoire Naturelle, Paris, France.

ABSTRACT **Metabolic interactions with endosymbiotic photosynthetic dinoflagellate *Symbiodinium* spp. are fundamental to reef-building corals (Scleractinia) thriving in nutrient-poor tropical seas. Yet, detailed understanding at the single-cell level of nutrient assimilation, translocation, and utilization within this fundamental symbiosis is lacking. Using pulse-chase ^{15}N labeling and quantitative ion microprobe isotopic imaging (NanoSIMS; nanoscale secondary-ion mass spectrometry), we visualized these dynamic processes in tissues of the symbiotic coral *Pocillopora damicornis* at the subcellular level. Assimilation of ammonium, nitrate, and aspartic acid resulted in rapid incorporation of nitrogen into uric acid crystals (after ~45 min), forming temporary N storage sites within the dinoflagellate endosymbionts. Subsequent intracellular remobilization of this metabolite was accompanied by translocation of nitrogenous compounds to the coral host, starting at ~6 h. Within the coral tissue, nitrogen is utilized in specific cellular compartments in all four epithelia, including mucus chambers, Golgi bodies, and vesicles in calicoblastic cells. Our study shows how nitrogen-limited symbiotic corals take advantage of sudden changes in nitrogen availability; this opens new perspectives for functional studies of nutrient storage and remobilization in microbial symbioses in changing reef environments.**

IMPORTANCE **The methodology applied, combining transmission electron microscopy with nanoscale secondary-ion mass spectrometry (NanoSIMS) imaging of coral tissue labeled with stable isotope tracers, allows quantification and submicrometric localization of metabolic fluxes in an intact symbiosis. This study opens the way for investigations of physiological adaptations of symbiotic systems to nutrient availability and for increasing knowledge of global nitrogen and carbon biogeochemical cycling.**

Received 21 January 2013 **Accepted** 16 April 2013 **Published** 14 May 2013

Citation Kopp C, Pernice M, Domart-Coulon I, Djediat C, Spangenberg JE, Alexander DTL, Hignette M, Meziane T, Meibom A. 2013. Highly dynamic cellular-level response of symbiotic coral to a sudden increase in environmental nitrogen. mBio 4(3):e00052-13. doi:10.1128/mBio.00052-13.

Invited Editor Victoria Orphan, Cal Tech **Editor** Margaret McFall-Ngai, University of Wisconsin

Address correspondence to C. Kopp, christophe.kopp@epfl.ch, or A. Meibom, anders.meibom@epfl.ch.

Fundamental to the highly biodiverse reef ecosystems in (sub)tropical coastal waters is the endosymbiotic relationship between scleractinian corals (Cnidaria; Anthozoa) and autotrophic unicellular dinoflagellate protists of the genus *Symbiodinium*, commonly known as zooxanthellae (1). The disruption of this mutualistic association (coral bleaching) in response to, e.g., anthropogenic ocean warming is widely considered a key factor in the decline of coral reefs worldwide (2). In oligotrophic (nutrient-poor) waters, which often characterize the tropics, the dinoflagellate endosymbionts supply their animal host with photosynthetically fixed carbon compounds (photosynthates) that are essential to their respiration, growth, reproduction, and skeletal calcification (3–5). The dinoflagellates are also involved in the acquisition and retention of dissolved inorganic and organic nitrogen (N) from the seawater in the form of ammonium (NH_4^+), nitrate (NO_3^-), dissolved free amino acids (DFAAs), and urea, with a preference for ammonium (6–8), but the details of this process are much less clear. Although increasing loads of dissolved N in coastal waters (i.e., nutrification) is thought to potentially perturb the symbiotic relationship and threaten coral health (9–11), details of the coral response to a sudden natural or anthropogenic change in environmental N availability are unclear, in particular with regard to (i) the precise cellular and subcellular sites of N acquisition and storage, (ii) the nature and turnover of N storage metabolites, and (iii) the spatial and temporal pattern of host-symbiont nitrogenous nutrient exchange and subsequent metabolic utilization in the symbiotic system.

Nanoscale secondary-ion mass spectrometry (NanoSIMS) isotopic imaging is a powerful analytical tool to simultaneously visualize and quantify *in situ* the incorporation and transfer of isotopically labeled metabolites in endosymbiotic organisms at subcellular-length scales (12–15). In this study, NanoSIMS anal-

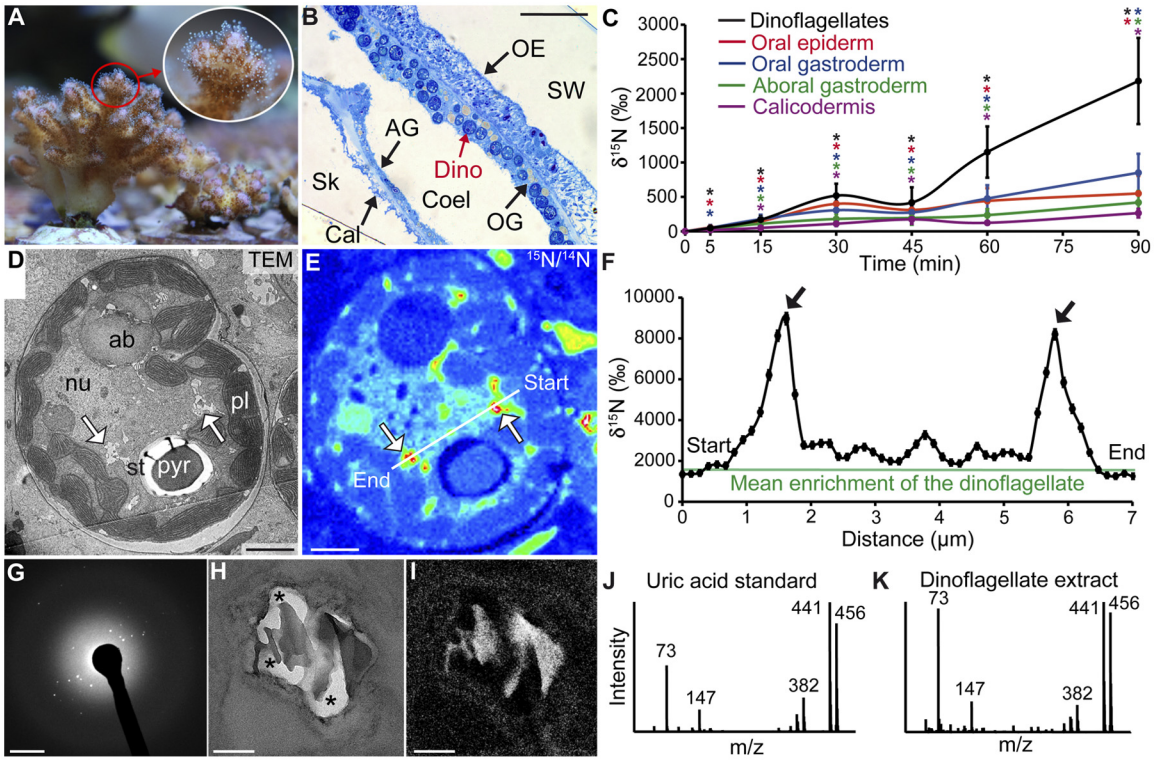

FIG 1 Nitrogen incorporation and storage within the coral-dinoflagellate endosymbiosis. (A) Coral nubbin (height, ~5 cm) of *P. damicornis*, showing individual polyps with extended tentacles (inset). (B) Optical image of a coral tissue section (methylene blue-Azur II staining) with abundant dinoflagellate cells (red arrow) in the oral gastroderm. Scale bar, 50 μm. SW, seawater; OE, oral epiderm; OG, oral gastroderm; Dino, dinoflagellate; Coel, coelenteron; AG, aboral gastroderm; Cal, calicodermis; Sk, skeleton. (C) NanoSIMS measurements of the dynamics of ^{15}N incorporation by the dinoflagellates and the four coral epithelia during 90 min of incubation with 20 μM [^{15}N]ammonium. Asterisks indicate significant incorporation of ^{15}N compared to that by the unlabeled control coral. TEM micrograph (D) and corresponding NanoSIMS isotopic $^{15}N/^{14}N$ image (E) of a dinoflagellate after 90 min of exposure to [^{15}N]ammonium. ^{15}N hot spots are spatially correlated with crystalline deposits (white arrows). Scale bar, 2 μm. ab, accumulation body; nu, nucleus; pl, plastid; pyr, pyrenoid; st, starch. (F) Variations of ^{15}N enrichment along the profile depicted in panel E passing through two ^{15}N hot spots (black arrows). Electron diffraction pattern (G) and corresponding zero-loss (elastically scattered) TEM micrograph (H) and N map (I) of a cluster of dinoflagellate crystalline inclusions. Scale bars, 2 nm^{-1} (G) and 100 nm (H and I). GC-MS spectra of a uric acid standard (J) and of uric acid from the dinoflagellates of *P. damicornis* (K).

ysis of coral tissue sections was combined with transmission electron microscopy (TEM) (the method is illustrated in Fig. S1 and Table S1 in the supplemental material) in order to investigate the dynamics of the assimilation and utilization of ^{15}N-labeled ammonium (NH_4^+), nitrate (NO_3^-), and DFAAs (here, aspartic acid) in the intact endosymbiosis between a reef-building coral and its dinoflagellates. Here, we define assimilation as the incorporation of N from inorganic and organic compounds initially dissolved in seawater into coral and dinoflagellate cell biomass. Pulse-chase labeling experiments with different N levels and multiple time scales (1- to 12-h pulse and 4-day chase) were performed at the Aquarium Tropical, Palais de la Porte Dorée (Paris, France), on coral nubbins of the very common and widely distributed Indo-Pacific reef-building coral species *Pocillopora damicornis* (16).

RESULTS

Ammonium assimilation—the first steps. To first characterize the cellular site of ammonium assimilation within the coral-dinoflagellate endosymbiosis, we incubated coral nubbins (Fig. 1A) in seawater containing [^{15}N]ammonium (20 μM, 90 min) and monitored the incorporation of the ^{15}N tracer into the dinoflagellate endosymbionts, which are exclusively located within the gastrodermal cells (mostly in the oral tissue layer), and in all four epithelia of the coral host tissue (Fig. 1B) as a function of time, using NanoSIMS isotopic imaging of tissue sections.

A rapid and simultaneous appearance of ^{15}N within both dinoflagellates and coral cells of all epithelia was observed (Fig. 1C), indicating that both symbiotic partners play a direct role in ammonium assimilation. ^{15}N enrichments significantly above the control level were detectable in both coral cells and dinoflagellates within 5 to 15 min after the beginning of the pulse (Fig. 1C), implying a rapid process of ammonium assimilation. Moreover, clear differences in the dynamics of ^{15}N incorporation were recorded between the dinoflagellates and the coral cells. After a 90-min incubation, the dinoflagellates were on average more enriched in ^{15}N (by a factor of 3.7) than the coral cells (Fig. 1C), demonstrating clearly that compared to their animal host, the dinoflagellates represent at the cellular level the most efficient site for ammonium assimilation. Note that during the pulse, coral cells in both oral tissue layers seemed to assimilate ammonium slightly faster than coral cells in both aboral tissue layers (Fig. 1C). Qualitatively similar results were obtained in a parallel experiment with coral nubbins incubated in a lower [^{15}N]ammonium concentration (2 μM, 4 h) (see Fig. S2 in the supplemental material). However, at this 2 μM dose, ammonium assimilation efficiencies

for both dinoflagellate and animal cells were lower by a factor of 4 to 5 than in the 20 μM experiment, suggesting a concentration-dependent effect for ammonium assimilation in both partners.

Nitrogen storage and remobilization by dinoflagellates. Figures 1D to F show that exposure to a pulse of [^{15}N]ammonium (20 μM, 90 min) resulted in the accumulation of ^{15}N into distinct hot spots in the dinoflagellate cells. These hot spots, easily identifiable in high-resolution NanoSIMS images (Fig. 1E), can have higher ^{15}N/^{14}N ratios (up to a factor of 5) than the average for dinoflagellates (Fig. 1F) and thus contribute strongly to the spatially heterogeneous ^{15}N distribution in dinoflagellates (see, e.g., Fig. 1E). The ^{15}N hot spots formed inside the dinoflagellates are colocalized with cytosolic crystalline structures, as indicated in the corresponding TEM image (Fig. 1D and E). The crystalline nature of these deposits was confirmed by TEM electron diffraction patterns (Fig. 1G). Moreover, electron energy loss spectroscopy (EELS) analyses and energy-filtered TEM (EFTEM) spectrum imaging showed that these crystals are N enriched compared to surrounding amorphous cellular material (Fig. 1H and I). Comparison with a synthetic uric acid standard (see Fig. S3 in the supplemental material) demonstrated that these crystals are indeed uric acid and ruled out other types of crystals, such as calcium oxalate. In parallel, gas chromatography-mass spectrometry (GC-MS) analyses confirmed the occurrence of uric acid molecules within the dinoflagellate cells (Fig. 1J and K; Fig. S4).

^{15}N accumulation into dinoflagellate uric acid crystals was also observed following a pulse of [^{15}N]nitrate (30 μM, 12 h) (Fig. S5A to S5C) and a pulse of DFAAs in the form of [^{15}N]aspartic acid (20 μM, 6 h) (Fig. S5D to S5F). For the latter experiment, aspartic acid assimilation was recorded at comparable efficiencies within the coral tissue, including all four epithelia, and the dinoflagellate endosymbionts (Fig. S5G).

Gas chromatography-combustion-isotope ratio mass spectrometry (GC-C-IRMS) unambiguously demonstrated the incorporation of ^{15}N into dinoflagellate uric acid following incubation with [^{15}N]ammonium at both high (20 μM, 90 min) and low (2 μM, 6 h) concentrations, as well as with [^{15}N]nitrate (30 μM, 12 h) (Table S2). The GC-C-IRMS results also suggested concentration-dependent ^{15}N incorporation into uric acid molecules (reaching ~900‰ in 1.5 h for 20 μM ammonium versus 6 h for 2 μM ammonium) (Table S2). Interestingly, the ^{15}N enrichment hot spots observed by NanoSIMS imaging are not associated solely with uric acid crystals; they are also associated with the lining of an amorphous electron-dense matrix of unknown composition enclosed in their single-membrane vesicles (Fig. S6).

Dynamic incorporation of N into uric acid crystals and subsequent remobilization are illustrated by the time sequence presented in Fig. 2. During a 1-h pulse of [^{15}N]ammonium (20 μM), ^{15}N becomes strongly incorporated into uric acid crystals after ~45 min (Fig. 2A to D). However, the ^{15}N enrichment of uric acid crystals is only temporary, as indicated by the gradual disappearance of ^{15}N hot spots inside the dinoflagellates, which was complete about 24 h after the beginning of the chase phase in seawater with a normal N-isotopic composition (Fig. 2E to J).

Nitrogen translocation from dinoflagellates to their coral host. Figure 3 shows the results of two parallel pulse (20 μM, 1 h) and chase (95 h) experiments with [^{15}N]ammonium. One experiment was carried out under standard light/dark (14 h/10 h) illumination conditions and the other under constant darkness with coral nubbins preacclimatized to darkness for 24 h. The objective of this preacclimatization to darkness was to inhibit the photosynthetically driven ammonium assimilation processes in the dinoflagellate cells (17) and, consequently, their potential translocation of nitrogenous material to their host. Figure 3A shows that, under standard light/dark illumination, both dinoflagellates and coral cells rapidly assimilated [^{15}N]ammonium during the pulse, with the dinoflagellates exhibiting greater efficiency, consistent with our previous observations (Fig. 1C). During the 95-h chase, however, the ^{15}N enrichments of both dinoflagellate and coral cells remained essentially constant (Fig. 3A). In contrast, under constant darkness, the dinoflagellates assimilated [^{15}N]ammonium at the same low level as the coral cells (Fig. 3B), which in general acquired less ^{15}N during the chase than under normal-illumination conditions (Fig. 3C). Thus, clear differences in ^{15}N enrichment of the coral cells between light/dark and constant darkness developed after about 6 h (Fig. 3C). With the caveat that under prolonged darkness, coral metabolism may be perturbed, this observation indicates the translocation of ^{15}N compounds from the photosynthetically active dinoflagellates to their coral host. Interestingly, coral cells in all oral and aboral epithelia benefited from this translocation (Fig. S7). Note that ^{15}N enrichments obtained for dinoflagellates from NanoSIMS imaging (Fig. 3A and B) are in good agreement with conventional isotope ratio mass spectrometry data for dinoflagellate bulk fractions separated from the same coral samples after tissue dissociation (Table S3), providing strong validation of the NanoSIMS *in situ* quantifications presented here.

Additional, direct evidence for N translocation between dinoflagellates and animal cells comes from [^{15}N]nitrate experiments. Indeed, because coral cells lack nitrate and nitrite reductase enzymes, nitrate is thought to be assimilated by dinoflagellates only (18, 19). Any nitrate-triggered ^{15}N enrichment in the coral cells can therefore be ascribed to translocation. Corals were first incubated for 12 h in light with [^{15}N]nitrate (30 μM) and then transferred for 84 h to unlabeled seawater under standard light/dark (14 h/10 h) cycling. Figure 4A shows that [^{15}N]nitrate was efficiently assimilated by the dinoflagellates during the pulse. In contrast, the ^{15}N labeling of the coral cells was detected only after 6 h into the pulse (Fig. 4A) and then steadily increased due to translocation of metabolites from the dinoflagellates. Translocation reached all oral and aboral cellular layers of the coral (Fig. S8), consistent with previous observations from experiments using ^{15}N-labeled ammonium (Fig. 3 and see Fig. S7 in the supplemental material). NanoSIMS isotopic imaging enabled us to further visualize and quantify the very first steps of N translocation from the dinoflagellates to their host gastroderm with relatively precise timing (Fig. 4B to F). After 2 h of incubation in [^{15}N]nitrate, only the dinoflagellates had incorporated ^{15}N, and the adjacent coral cells were unlabeled (Fig. 4B). But from 6 h into the pulse, enhanced ^{15}N levels were clearly detected in coral cells as metabolites began to translocate (Fig. 4C and D). Translocation then continued during the 84-h chase period (Fig. 4E and F). Together, our results from both [^{15}N]ammonium and [^{15}N]nitrate experiments therefore indicate a time lag of about 6 h between the onset of the pulse of dissolved inorganic N and the beginning of N translocation from dinoflagellates to the host. For both ammonium and nitrate experiments performed under a normal photoperiod, the ^{15}N enrichment of dinoflagellates was not clearly observed to diminish during the 4-day chase (Fig. 3A and 4A). At the same time,

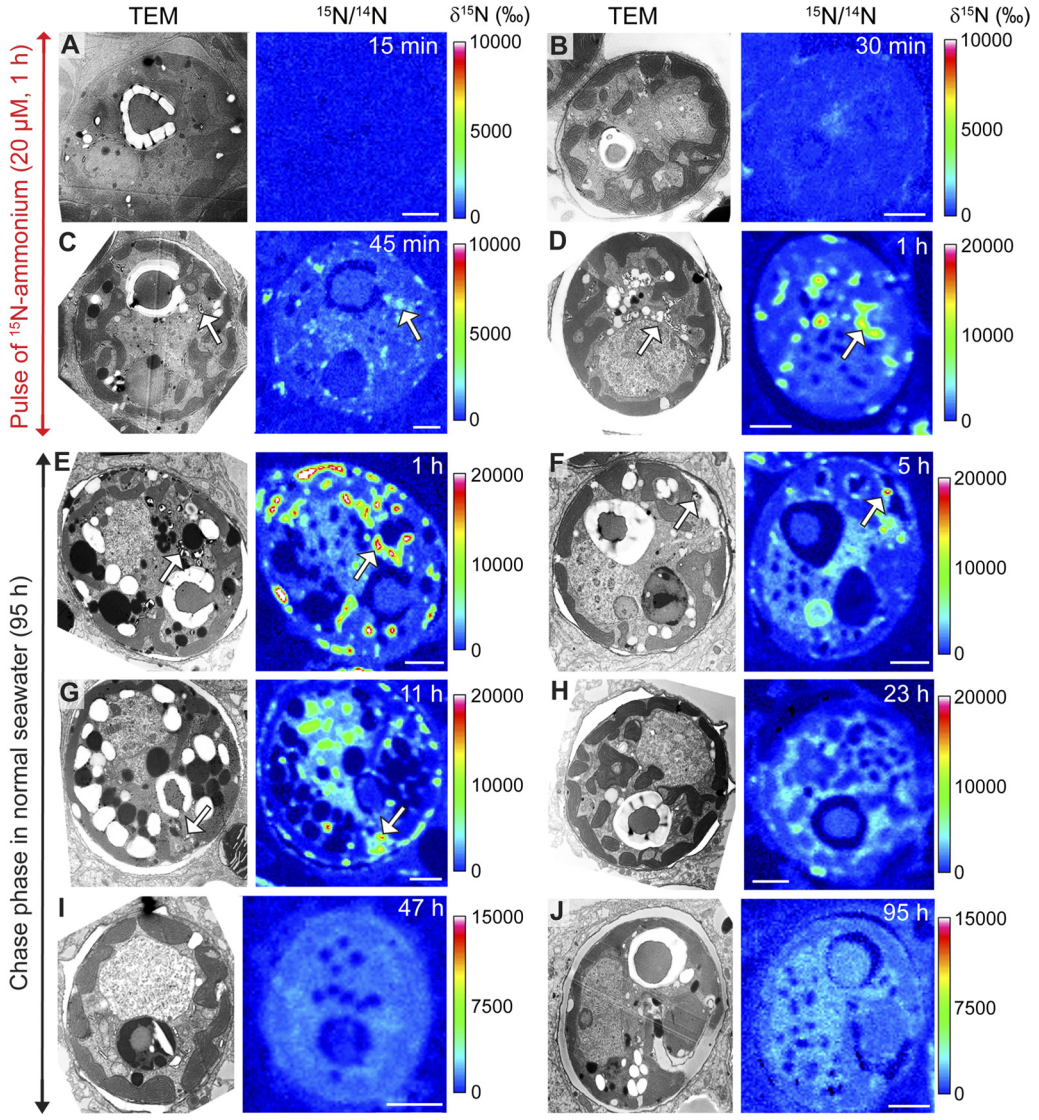

FIG 2 Dynamics of N storage and remobilization in the dinoflagellates. Each panel represents a TEM image of a dinoflagellate (left) and its corresponding $^{15}N/^{14}N$ NanoSIMS image (right), obtained at 15 min (A), 30 min (B), 45 min (C), and 60 min (D) of coral incubation in 20 μM [^{15}N]ammonium (pulse phase) and after 1 h (E), 5 h (F), 11 h (G), 23 h (H), 47 h (I), and 95 h (J) of subsequent coral incubation in unlabeled seawater (chase phase). White arrows indicate highly labeled crystalline uric acid inclusions in the dinoflagellates. Scale bar, 2 μm.

there is clear evidence for N translocation to the coral host. The dinoflagellates probably constitute relatively large N reservoirs (Fig. S1B) that do not become substantially depleted by translocation of N to the coral host on these short time scales.

Subcellular sites of nitrogen utilization in the coral host. Combined TEM and NanoSIMS findings exhibited in Fig. 5 show the subcellular sites of coral host utilization of N either acquired directly by the host or translocated from the dinoflagellates at different times during a pulse-chase experiment with [^{15}N]ammonium (20 μM, 1-h pulse, 95-h chase). (i) Under standard light/dark cycling, ^{15}N was observed to accumulate within small compartments (loculae) of mucus chambers in glandular cells (mucocytes) of the oral surface epithelia after 12 h (Fig. 5A to D). In contrast, during the constant-darkness experiment (described above), no ^{15}N labeling of mucocytes was detected by NanoSIMS imaging. (ii) During both standard light/dark cycling and constant darkness, ^{15}N was observed to accumulate within Golgi bodies of the coral cells in all epithelia, suggesting assimilation into proteins. Figure 5E to H provide illustrations of N accumulation at 45 min of incubation with [^{15}N]ammonium. (iii) Under standard light/dark cycling, ^{15}N was observed to accumulate in the calicodermis epithelia within vesicles (~300 to 400 nm in diameter) with a granular content (Fig. 5I to L) at 6 h into the experiment.

Note that monitoring of the dinoflagellate mitotic index in dissociated tissue suspensions prepared at different times during a pulse-chase experiment with [^{15}N]ammonium (20 μM, 1-h pulse, 95-h chase) indicated that dinoflagellates did not use assimilated N to actively proliferate on these short time scales (data not shown).

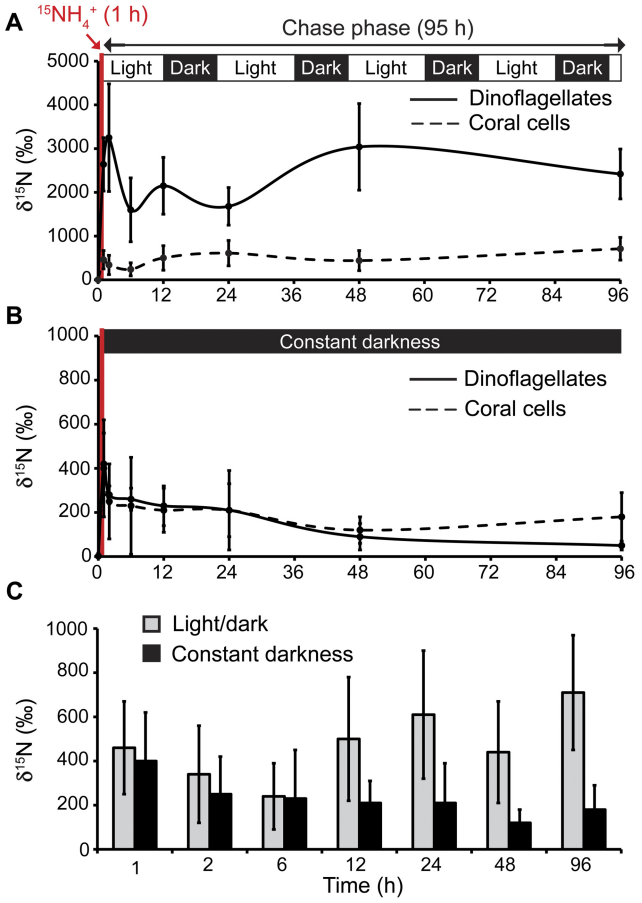

FIG 3 Ammonium assimilation and N translocation from the dinoflagellates to the coral tissue. NanoSIMS measurements of ^{15}N partitioning between dinoflagellates and coral tissue during the 95-h chase phase under standard light/dark (14 h/10 h) cycling, following a 1-h pulse-labeling in light with [^{15}N]ammonium (20 μM) (A) and during a 95-h chase phase under constant darkness, following a 1 h pulse-labeling in darkness with [^{15}N]ammonium (20 μM) (corals were preacclimatized to darkness for 24 h) (B). (C) Comparison of coral host ^{15}N enrichment levels between the two experimental conditions.

DISCUSSION

The ability of symbiotic reef corals to take up and assimilate various forms of inorganic (ammonium, nitrate) and organic (dissolved free amino acids, urea) N dissolved in the ambient seawater is well recognized, with ammonium representing the preferential source (6–8). However, the relative contribution to ammonium acquisition of each partner of the coral-dinoflagellate endosymbiosis has remained an open question (8). On one hand, early nutrient depletion experiments pointed to the dinoflagellates as the main assimilation site (17, 20), a conclusion later supported by bulk-level tracer studies with [^{15}N]ammonium (21–24). The glutamine synthetase (GS)-glutamine oxoglutarate aminotransferase (GOGAT) enzymatic pathway was thus proposed as the main mechanism for ammonium assimilation by dinoflagellates, a view strongly supported by enzyme inhibitor experiments, with, e.g., the GS inhibitor methionine sulfoximine (MSX) (25) or the GOGAT inhibitor azaserine (26). On the other hand, detection within cnidarian animal tissue of both GS and glutamate dehydrogenase (GDH) indicates that the host potentially also has the enzymatic machinery for ammonium assimilation (26–28). Therefore, a host-mediated model of ammonium assimilation in which the animal host is the primary site for ammonium incorporation was proposed (29).

A previous short-term pulse-chase (12 h) experiment with [^{15}N]ammonium, combining TEM and *in situ* quantitative NanoSIMS isotopic imaging of thick tissue sections (250 nm), indicated a primary role for dinoflagellates in ammonium assimilation compared to that of coral cells of the two epithelia in the oral tissue of the reef coral *Acropora aspera* (15). The present work confirms and expands this conclusion for the symbiotic reef coral *P. damicornis*, in which both dinoflagellate and coral cells, including all four coral epithelia (in oral and aboral tissue), are directly implicated in ammonium assimilation, with preferential incorporation by the dinoflagellate endosymbionts. Interestingly, ammonium assimilation by the symbiotic system appears less rapid in the present *P. damicornis* coral than in the previously studied *A. aspera* (15). Such kinetic differences may reflect variations of environmental parameters and/or species-specific effects and should be addressed in future experiments.

Note that by comparing two different ammonium concentrations (20 μM versus 2 μM), our observations suggest a concentration-dependent mechanism for ammonium assimilation within both dinoflagellate and coral cells, a response previously identified only for the dinoflagellate endosymbionts of cnidarians (17, 20, 23). The apparent differences in the dynamics of ammonium incorporation between oral and aboral cellular layers of *P. damicornis* coral might be explained by various factors, including (i) different activities of ammonium-assimilatory enzymes among coral epithelia, (ii) different means of access of coral epithelia to [^{15}N]ammonium transported from seawater, i.e., by the oral tissue facing seawater versus the aboral tissue facing the skeleton, or (iii) the greater density of dinoflagellates in oral tissue, because these endosymbionts are thought to drive the uptake of ammonium from seawater (6).

Additionally, we confirmed by NanoSIMS isotopic analyses that nitrate assimilation from seawater by the coral-dinoflagellate symbiosis takes place exclusively in the endosymbiotic cells, which possess nitrate- and nitrite reductase-assimilatory enzymes (18, 19). Moreover, our NanoSIMS analyses indicate that aspartic acid dissolved in seawater is assimilated with similar efficiencies in the light by dinoflagellates and coral cells of all four epithelia, supporting previous observations from bulk-level tracer studies with ^{15}N-labeled DFAAs in various symbiotic cnidarians (7, 22). Of interest, this conclusion strongly contrasts with early autoradiographic investigations performed on cnidarian tissue sections at the light microscopy level, proposing that incorporation of tritiated DFAAs occurred primarily in the oral epiderm rather than the oral gastroderm, with no incorporation of DFAAs into the dinoflagellates (30, 31). These divergent results could be explained by the higher sensitivity and spatial resolution of NanoSIMS, which allows more precise, subcellular characterization of the sites for N assimilation. Aspartic acid is a major amino acid component of biocarbonate skeletal organic matrices (32). It is also involved in the purine pathway for uric acid metabolism (33). The observed contribution of dinoflagellate endosymbionts to its assimilation supports their potential role in providing precursors of skeletal organic matrix to fuel the biocalcification of their host.

The coastal areas of the (sub)tropical oceans are characterized by large N concentration fluctuations due to, e.g., runoff from

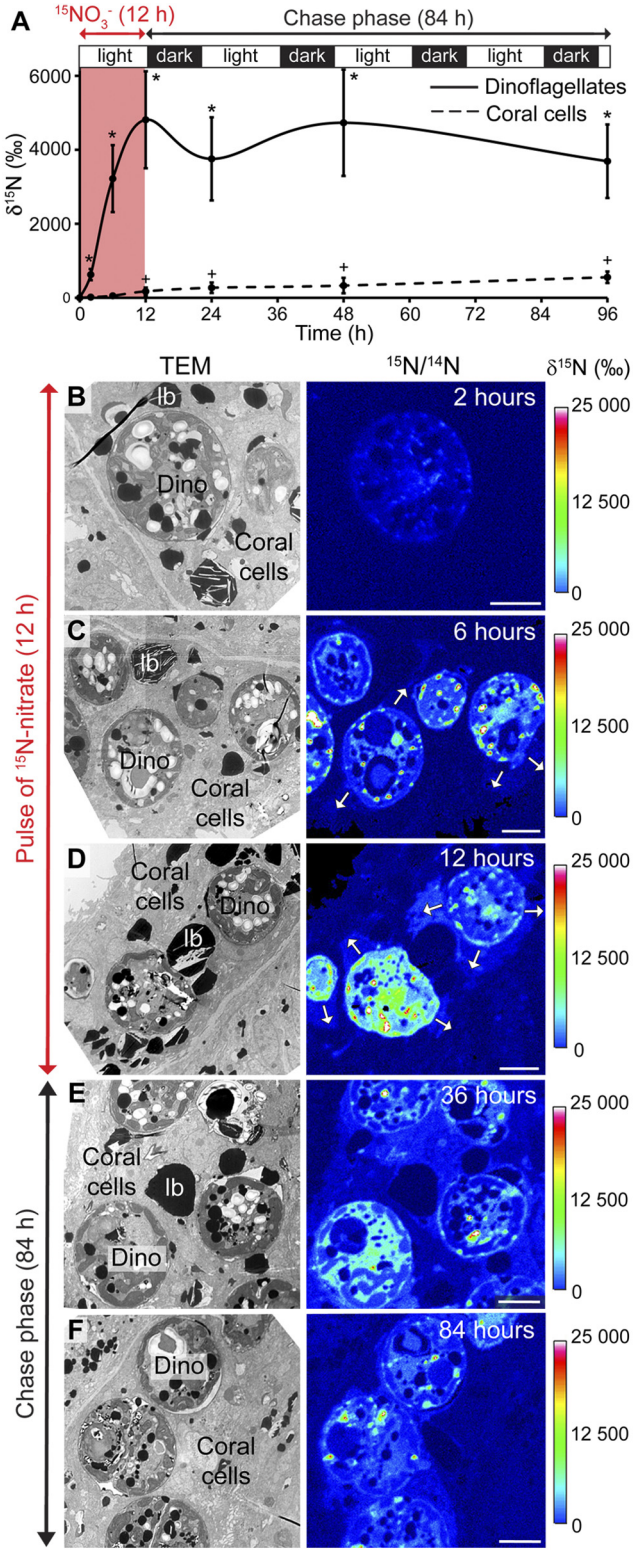

FIG 4 Nitrate assimilation by the dinoflagellates and N translocation to their coral host. (A) NanoSIMS measurements of ^{15}N partitioning between dinoflagellates and coral tissue during an 84-h chase under standard light/dark (14 h/10 h) cycling, following a 12-h pulse (30 μM) of [^{15}N]nitrate labeling in light. Significant labeling is indicated for the dinoflagellates (*) and the coral host tissue (+) compared to that of the unlabeled control corals. (B to F) TEM micrographs (left) and corresponding NanoSIMS isotopic $^{15}N/^{14}N$ images

(Continued)

agricultural lands, sewage effluents, groundwater discharge, or fish excretion (10, 11, 34). A mechanism for temporary N storage in uric acid crystals in dinoflagellate cells has high nutritional importance for their coral host in such N-fluctuating environments; in addition, a central role has been demonstrated for endosymbiotic dinoflagellates in the rapid assimilation of dissolved N from ambient seawater. Macro- and microalgae are known to be capable of rapid assimilation and storage of N, which is then mobilized for growth during subsequent periods of N deficiency (35–37). Dinoflagellate crystalline deposits, previously assumed to be calcium oxalate (38), have recently been identified as uric acid ($C_5H_4N_4O_3$) in the sea anemone *Aiptasia* sp. and were hypothesized to be subcellular sites for temporary N storage (39). Here, we demonstrate that in scleractinian corals, endosymbiotic dinoflagellates respond to a sudden increase in dissolved inorganic (ammonium, nitrate) and organic (aspartic acid) N in ambient seawater by storing N rapidly in intracellular uric acid crystals. Moreover, we demonstrate the rapid turnover of this metabolite, likely mobilized for maintaining the N status of the coral-dinoflagellate association under nutrient-limited environments (39).

The formation and further remobilization of uric acid crystals are also reported (i) in other endosymbiotic associations involving marine animal hosts, such as in the tripartite endosymbiosis between the tunicate *Molgula manhattensis*, its apicomplexan *Nephromyces* protist (phylogenetically related to the dinoflagellates, in the Alveolates supertaxon), and their symbiotic intracellular bacteria (40–42), and (ii) in the endosymbiosis between the acoel flatworm *Symsagittifera roscoffensis* and the green microalgae *Tetraselmis convolutae* (43). However, in these associations, unlike with our results with symbiotic corals, it is the host partner that produces uric acid deposits as transitory N stores, which are later remobilized through the uricolytic activity of their endosymbionts.

The dynamic pattern of uric acid production and remobilization that we have observed within dinoflagellate endosymbionts of scleractinian corals is likely to reflect the presence and activities of enzymes involved in *de novo* purine biosynthesis and further catabolism. Similar metabolic processes have been documented in the terrestrial endosymbiosis between leguminous plants and N_2-fixing bacteria, which involves storage and subsequent conversion of uric acid into ureides (33, 44). In the latter symbiotic system, bacteria convert atmospheric N_2 into ammonium, which is transferred to the plant host, where *de novo* purine biosynthesis and purine catabolism yield uric acid. Its subsequent metabolization into ureides (allantoin and allantoate) allocated to the entire host organism supports the plant N requirements. Our BLAST (45) analyses (Table S4) of *Symbiodinium* expressed sequence tags (ESTs) (http://medinalab.org/zoox/) indicate that transcripts encoding enzymes essential to purine synthesis and remobilization are present in the *Symbiodinium* transcriptome. This includes xanthine dehydrogenase (46), which catalyzes the conversion of hypoxanthine and xanthine to uric acid and uricase (19), which is

Figure Legend Continued

(right) of the dinoflagellate-containing oral gastroderm at 2, 6, and 12 h in the pulse (panels B, C, and D, respectively) and at 36 and 84 h in the chase (panels E and F, respectively). White arrows highlight nitrogenous compounds transferred from the dinoflagellates to their adjacent coral cells during the pulse. Scale bar, 5 μm. lb, coral lipid bodies; Dino, dinoflagellate.

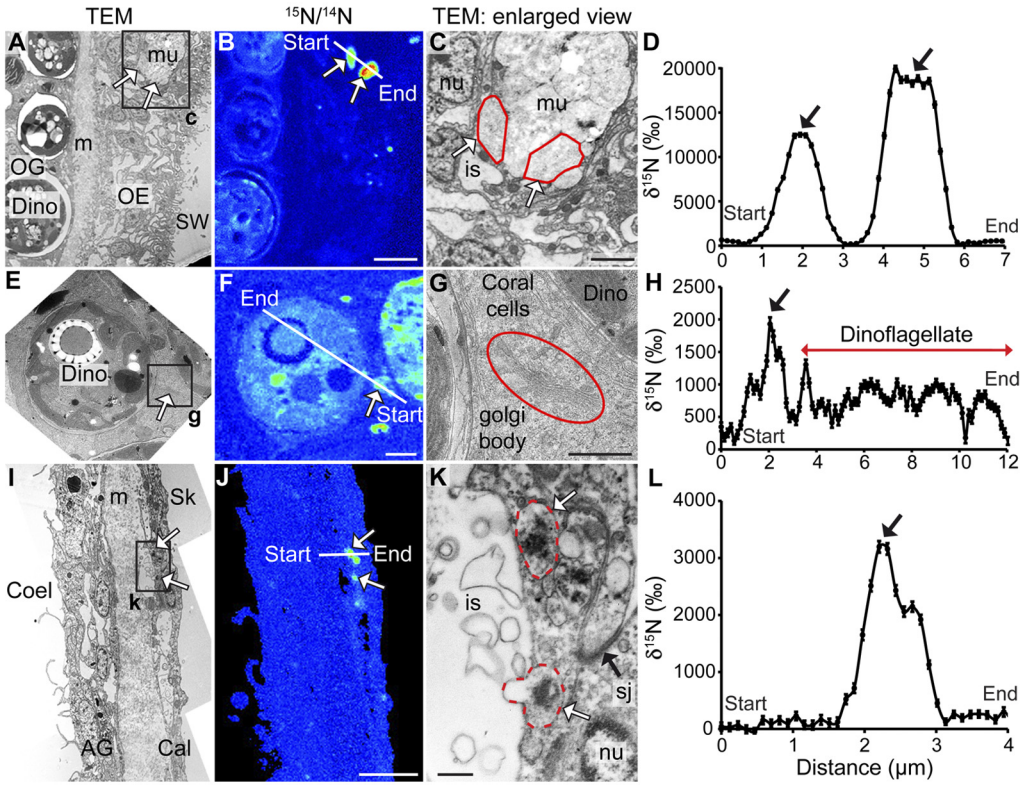

FIG 5 Coral host utilization of N assimilated from [^{15}N]ammonium under light/dark conditions. TEM micrograph (A) and corresponding NanoSIMS isotopic ^{15}N/^{14}N image (B) of the oral epiderm 11 h into the chase phase, showing ^{15}N accumulation in mucus chambers of a mucocyte (white arrows). Scale bar, 5 μm. (C) High-magnification TEM view of the labeled structures (loculae). Scale bar, 2 μm. (D) ^{15}N quantification of the profile indicated in panel B. TEM micrograph (E) and corresponding NanoSIMS isotopic ^{15}N/^{14}N image (F) of the oral gastroderm 45 min into the pulse (under light), showing ^{15}N accumulation in a Golgi body (white arrows). Scale bar, 2 μm. (G) High-magnification TEM view of the labeled structure. Scale bar, 1 μm. (H) ^{15}N quantification of the profile indicated in panel F. TEM micrograph (I) and corresponding NanoSIMS isotopic ^{15}N/^{14}N image (J) of the aboral epithelia 5 h into the chase phase, showing ^{15}N accumulation in calicoblastic cells (white arrows). Scale bar, 5 μm. (K) High-magnification TEM view of the calicoblastic cell showing ^{15}N incorporation in large vesicles (white arrows). Scale bar, 500 nm. (L) ^{15}N quantification of the profile indicated in panel J. OE, oral epiderm; OG, oral gastroderm; AG, aboral gastroderm; Cal, calicodermis; Coel, coelenteron; Dino, dinoflagellate; is, intercellular space; m, mesoglea; mu, mucocyte; nu, nucleus; sj, septate junction; Sk, skeleton; SW, seawater.

involved in the subsequent oxidation of uric acid to the ureide allantoin. Our results therefore provide new evidence strengthening the hypothesis that activation of purine-related metabolic pathways is involved in controlling the N bio-economy of cnidarian endosymbioses under N-fluctuating marine environments (39).

In reef corals, endosymbiotic dinoflagellate cells are thought to substantially contribute to the N requirements of their host by translocating N-bearing compounds in the form of amino acids (47, 48) and/or larger N-containing glycoconjugates (49, 50). However, direct evidence for this nutrient exchange, as well as its spatial pattern within the tissue layers and its precise timing, remained unclear (51). Here, combined TEM and NanoSIMS isotopic imaging of tissue sections provide direct *in situ* visualization and quantification of the dynamics of N fluxes in the symbiotic reef coral *P. damicornis*. Nitrogen translocation occurs first in the dinoflagellate-containing oral gastroderm about 6 h after exposure to a dissolved ^{15}N-labeled tracer. Subsequently, the three other cellular layers receive translocated N, indicating exchange between the different coral epithelia. Interestingly, the observed 6-h time lag is consistent with the hypothesis for delayed N release by the endosymbiotic dinoflagellates (52). Ultrastructural observations of the subcellular sites of coral host utilization of N acquired either directly by the host or translocated from the dinoflagellates suggest N utilization for important physiological functions of the coral, such as synthesis of mucus, proteins, and potential precursors of the skeletal organic matrix, known to be involved in coral biomineralization processes (53).

In conclusion, by combining pulse-chase experiments using ^{15}N-enriched ammonium, nitrate, and aspartic acid with TEM ultrastructural observations and NanoSIMS isotopic imaging of thin coral tissue sections, we visualized and quantified *in situ* at the subcellular level the dynamics of dissolved N acquisition, storage, and utilization by the coral-dinoflagellate endosymbiosis. In particular, we provide experimental evidence for temporary N storage in dinoflagellate uric acid crystals in response to fluctuating environmental dissolved-nitrogen availability. In the context of marine environmental change due to both anthropogenic activities and natural fluctuations (e.g., ocean warming, acidification, pollution, and nutrification), this approach has the potential to provide new insights about how coral reef ecosystems will respond to such environmental perturbations.

MATERIALS AND METHODS

The pulse-chase experiments using ^{15}N-enriched ammonium, nitrate, and aspartic acid (obtained from Sigma-Aldrich) were carried out with small nubbins (~5 cm in height) of the scleractinian coral *Pocillopora damicornis* (Linnaeus, 1758) growing at the Aquarium Tropical, Palais de la Porte Dorée (Paris, France). The nubbins were prepared from one large colony and acclimatized for 8 weeks in artificial seawater (Instant Ocean salts) with low nutrient concentrations (NO_2^-, <1 μM; NH_4^+, <1 μM; PO_4^{3-}, <1 μM), except for NO_3^- (~30 to 40 μM, due to seawater equilibration in a large fish-containing tank). The temperature was 25 ± 1°C, salinity was 32 ± 1‰, the pH was 8.1 ± 0.1, and the photoperiod was 14 h of light and 10 h of dark. Corals were not fed with plankton during the acclimatization period and the subsequent experiments. For labeling pulses with ^{15}N tracers, 0.2 μm filtered seawater was used, except for the [^{15}N]nitrate pulse, for which freshly prepared artificial seawater with a low NO_3^- concentration was used. The chase was carried out in seawater with a normal isotopic abundance. Detailed descriptions of the experimental design are provided in the supplemental material (Text S1).

Transmission electron microscopy of coral tissue (70-nm-thick resin sections) was performed after conventional primary chemical fixation with aldehydes (glutaraldehyde and formaldehyde) and secondary chemical fixation with osmium tetroxide.

For NanoSIMS isotopic imaging and quantification, the exact same areas of interest selected by TEM observations were analyzed with a NanoSIMS ion microprobe. Data were processed using the L'IMAGE software. Regions of interest (ROIs) were defined from the $^{15}N/^{14}N$ images to quantify the bulk ^{15}N enrichment of the dinoflagellates and of cells in the four epithelia composing the coral tissue. Similar tissue positions in the coenosarc and upper part of the polyp (coenosarc-polyp transition area) were selected for all TEM and NanoSIMS analyses.

Selected-area electron diffraction, EELS, and EFTEM spectrum imaging for crystallinity assessment of intracellular deposits and mapping of elemental N were performed using a JEOL 2200FS TEM instrument with an in-column Ω filter.

Identification of uric acid in dinoflagellate water extracts was performed by GC-MS analysis of the trimethylsilyl derivatives and by comparison of the retention times and mass spectra with those of a commercial uric acid standard. The ^{15}N isotopic enrichment in dinoflagellate uric acid extracted from corals exposed to various ^{15}N-labeled compounds was measured by GC-C-IRMS.

Detailed methods for TEM ultrastructural observations, NanoSIMS isotopic imaging, and bulk N-isotopic analyses of the dinoflagellate fraction, as well as for electron diffraction, EFTEM spectrum imaging, and EELS of uric acid crystals and metabolite-specific GC-MS and GC-C-IRMS analyses of uric acid are provided in the supplemental material (Text S1).

SUPPLEMENTAL MATERIAL

Supplemental material for this article may be found at http://mbio.asm.org/lookup/suppl/doi:10.1128/mBio.00052-13/-/DCSupplemental.

Text S1, PDF file, 0.2 MB.
Figure S1, JPG file, 0.4 MB.
Figure S2, JPG file, 0.2 MB.
Figure S3, JPG file, 0.5 MB.
Figure S4, JPG file, 0.8 MB.
Figure S5, JPG file, 0.7 MB.
Table S1, PDF file, 0.2 MB.
Table S2, PDF file, 0.2 MB.
Table S3, PDF file, 0.1 MB.
Table S4, PDF file, 0.1 MB.

ACKNOWLEDGMENTS

This work was supported in part by European Research Council advanced grant 246749 (BioCarb), Swiss National Science Foundation grant CR23I2_141048, CNRS grant PIR Interface 2010 (NanoSIMS and symbiosis), and an MNHN-ATM grant (Biomineralization).

We owe special thanks to the technical staff at the Aquarium Tropical, Palais de la Porte Dorée, in Paris for highly professional assistance with coral manipulation and aquarium maintenance, to Najet Thiney for sample preparations, and to Géraldine Toutirais and Cyrielle Sophie for technical assistance with electron microscopy. Guillaume Lucas is thanked for scripting of Principal Component Analysis (PCA) in DigitalMicrograph.

REFERENCES

1. **Davy SK, Allemand D, Weis VM.** 2012. Cell biology of cnidarian-dinoflagellate symbiosis. Microbiol. Mol. Biol. Rev. **76**:229–261.
2. **Hoegh-Guldberg O.** 1999. Climate change, coral bleaching and the future of the world's coral reefs. Mar. Freshw. Res. **50**:839–866.
3. **Falkowski PG, Dubinsky Z, Muscatine L, Porter JW.** 1984. Light and the bioenergetics of a symbiotic coral. BioScience **34**:705–709.
4. **Muscatine L.** 1990. The role of symbiotic algae in carbon and energy flux in reef corals. Ecosyst. World **25**:75–87.
5. **Tremblay P, Grover R, Maguer JF, Legendre L, Ferrier-Pagès C.** 2012. Autotrophic carbon budget in coral tissue: a new 13C-based model of photosynthate translocation. J. Exp. Biol. **215**:1384–1393.
6. **D'Elia C, Domotor S, Webb K.** 1983. Nutrient uptake kinetics of freshly isolated zooxanthellae. Mar. Biol. **75**:157–167.
7. **Grover R, Maguer JF, Allemand D, Ferrier-Pagès C.** 2008. Uptake of dissolved free amino acids by the scleractinian coral *Stylophora pistillata*. J. Exp. Biol. **211**:860–865.
8. **Yellowlees D, Rees TA, Leggat W.** 2008. Metabolic interactions between algal symbionts and invertebrate hosts. Plant Cell Environ. **31**:679–694.
9. **Koop K, Booth D, Broadbent A, Brodie J, Bucher D, Capone D, Coll J, Dennison W, Erdmann M, Harrison P, Hoegh-Guldberg O, Hutchings P, Jones GB, Larkum AW, O'Neil J, Steven A, Tentori E, Ward S, Williamson J, Yellowlees D.** 2001. ENCORE: the effect of nutrient enrichment on coral reefs. Synthesis of results and conclusions. Mar. Pollut. Bull. **42**:91–120.
10. **Szmant AM.** 2002. Nutrient enrichment on coral reefs: is it a major cause of coral reef decline? Estuaries **25**:743–766.
11. **Fabricius KE.** 2005. Effects of terrestrial runoff on the ecology of corals and coral reefs: review and synthesis. Mar. Pollut. Bull. **50**:125–146.
12. **Lechene C, Hillion F, McMahon G, Benson D, Kleinfeld AM, Kampf JP, Distel D, Luyten Y, Bonventre J, Hentschel D, Park KM, Ito S, Schwartz M, Benichou G, Slodzian G.** 2006. High-resolution quantitative imaging of mammalian and bacterial cells using stable isotope mass spectrometry. J. Biol. **5**:20–30.
13. **Lechene CP, Luyten Y, McMahon G, Distel DL.** 2007. Quantitative imaging of nitrogen fixation by individual bacteria within animal cells. Science **317**:1563–1566.
14. **Clode PL, Stern RA, Marshall AT.** 2007. Subcellular imaging of isotopically labeled carbon compounds in a biological sample by ion microprobe (NanoSIMS). Microsc. Res. Tech. **70**:220–229.
15. **Pernice M, Meibom A, Van Den Heuvel A, Kopp C, Domart-Coulon I, Hoegh-Guldberg O, Dove S.** 2012. A single-cell view of ammonium assimilation in coral-dinoflagellate symbiosis. ISME J. **6**:1314–1324.
16. **Veron J.** 2000. Corals of the world. Australian Institute of Marine Science, Townsville, Australia.
17. **Muscatine L, D'Elia C.** 1978. The uptake, retention, and release of ammonium by reef corals. Limnol. Oceanogr. **23**:725–734.
18. **Crossland C, Barnes D.** 1977. Nitrate assimilation enzymes from two hard corals, *Acropora acuminata* and *Goniastrea australensis*. Comp. Biochem. Physiol. B Biochem. Mol. Biol. **57**:151–157.
19. **Leggat W, Hoegh-Guldberg O, Dove S, Yellowlees D.** 2007. Analysis of an EST library from the dinoflagellate (Symbiodinium sp.) symbiont of reef-building corals. J. Phycol. **43**:1010–1021.
20. **Wilkerson FP, Muscatine L.** 1984. Uptake and assimilation of dissolved inorganic N by a symbiotic sea anemone. Proc. R. Soc. Lond. B Biol. Sci. **221**:71–86.
21. **Roberts J, Davies P, Fixter L, Preston T.** 1999. Primary site and initial products of ammonium assimilation in the symbiotic sea anemone *Anemonia viridis*. Mar. Biol. **135**:223–236.
22. **Wilkerson FP, Kremer P.** 1992. DIN, DON and PO4 flux by a medusa with algal symbionts. Mar. Ecol. Prog. Ser. **90**:237–250.
23. **Grover R, Maguer JF, Reynaud-Vaganay S, Ferrier-Pagès C.** 2002. Uptake of ammonium by the scleractinian coral *Stylophora pistillata*: effect of feeding, light, and ammonium concentrations. Limnol. Oceanogr. **47**:782–790.

24. **Lipschultz F, Cook C.** 2002. Uptake and assimilation of 15N-ammonium by the symbiotic sea anemones *Bartholomea annulata* and *Aiptasia pallida*: conservation versus recycling of nitrogen. Mar. Biol. **140**:489–502.
25. **Anderson S, Burris J.** 1987. Role of glutamine synthetase in ammonia assimilation by symbiotic marine dinoflagellates (zooxanthellae). Mar. Biol. **94**:451–458.
26. **Rahav O, Dubinsky Z, Achituv Y, Falkowski P.** 1989. Ammonium metabolism in the zooxanthellate coral, *Stylophora pistillata*. Proc. R. Soc. Lond. B **236**:325–337.
27. **Yellowlees D, Rees T, Fitt W.** 1994. Effect of ammonium-supplemented seawater on glutamine synthetase and glutamate dehydrogenase activities in host tissue and zooxanthellae of *Pocillopora damicornis* and on ammonium uptake rates of the zooxanthellae. Pac. Sci. **48**:291–295.
28. **Wang J, Douglas AE.** 1998. Nitrogen recycling or nitrogen conservation in an alga-invertebrate symbiosis? J. Exp. Biol. **201**:2445–2453.
29. **Miller D, Yellowlees D.** 1989. Inorganic N uptake by symbiotic marine cnidarians: a critical review. Proc. R. Soc. Lond. B Biol. Sci. **237**:109–125.
30. **Goreau TF, Goreau NI, Yonge C.** 1971. Reef corals: autotrophs or heterotrophs? Biol. Bull. **141**:247–260.
31. **Schlichter D.** 1982. Nutritional strategies of cnidarians: the absorption, translocation and utilization of dissolved nutrients by *Heteroxenia fuscescens*. Am. Zool. **22**:659–669.
32. **Puverel S, Tambutté E, Pereira-Mouriès L, Zoccola D, Allemand D, Tambutté S.** 2005. Soluble organic matrix of two Scleractinian corals: partial and comparative analysis. Comp. Biochem. Physiol. B Biochem. Mol. Biol. **141**:480–487.
33. **Smith PMC, Atkins CA.** 2002. Purine biosynthesis. Big in cell division, even bigger in nitrogen assimilation. Plant Physiol. **128**:793–802.
34. **Meyer JL, Schultz ET, Helfman GS.** 1983. Fish schools: an asset to corals. Science **220**:1047–1049.
35. **Rosenberg C, Ramus J.** 1982. Ecological growth strategies in the seaweeds *Gracilaria foliifera* (Rhodophyceae) and *Ulva* sp. (Chlorophyceae): soluble N and reserve carbohydrates. Mar. Biol. **66**:251–259.
36. **Fujita RM, Wheeler PA, Edwards RL.** 1989. Assessment of macroalgal N limitation in a seasonal upwelling region. Mar. Ecol. Prog. Ser. **53**: 293–303.
37. **Bode A, Botas J, Fernandez E.** 1997. Nitrate storage by phytoplankton in a coastal upwelling environment. Mar. Biol. **129**:399–406.
38. **Taylor D.** 1968. In situ studies on the cytochemistry and ultrastructure of a symbiotic marine dinoflagellate. J. Mar. Biol. Assoc. UK **48**:349–366.
39. **Clode PL, Saunders M, Maker G, Ludwig M, Atkins CA.** 2009. Uric acid deposits in symbiotic marine algae. Plant Cell Environ. **32**:170–177.
40. **Saffo MB.** 1988. Nitrogen waste or nitrogen source? Urate degradation in the renal sac of molgulid tunicates. Biol. Bull. **175**:403–409.
41. **Saffo MB.** 1990. Symbiosis within a symbiosis: intracellular bacteria within the endosymbiotic protist Nephromyces. Mar. Biol. **107**:291–296.
42. **Saffo MB, McCoy AM, Rieken C, Slamovits CH.** 2010. Nephromyces, a beneficial apicomplexan symbiont in marine animals. Proc. Natl. Acad. Sci. USA **107**:16195.
43. **Douglas AE.** 1983. Uric acid utilization in *Platymonas convolutae* and symbiotic *Convoluta roscoffensis*. J. Mar. Biol. Assoc. UK **63**:435–447.
44. **Werner AK, Witte CP.** 2011. The biochemistry of nitrogen mobilization: purine ring catabolism. Trends Plant Sci. **16**:381–387.
45. **Altschul SF, Gish W, Miller W, Myers EW, Lipman DJ.** 1990. Basic local alignment search tool. J. Mol. Biol. **215**:403–410.
46. **Bayer T, Aranda M, Sunagawa S, Yum LK, Desalvo MK, Lindquist E, Coffroth MA, Voolstra CR, Medina M.** 2012. Symbiodinium transcriptomes: genome insights into the dinoflagellate symbionts of reef-building corals. PLoS One **7**:e35269. http://dx.doi.org/10.1371/journal.pone.0035269.
47. **Muscatine L, Cernichiari E.** 1969. Assimilation of photosynthetic products of zooxanthellae by a reef coral. Biol. Bull. **137**:506–523.
48. **Sutton D, Hoegh-Guldberg O.** 1990. Host-zooxanthella interactions in four temperate marine invertebrate symbioses: assessment of effect of host extracts on symbionts. Biol. Bull. **178**:175–186.
49. **Markell DA, Trench RK.** 1993. Macromolecules exuded by symbiotic dinoflagellates in culture: amino acid and sugar composition. J. Phycol. **29**:64–68.
50. **Markell DA, Wood-Charlson EM.** 2010. Immunocytochemical evidence that symbiotic algae secrete potential recognition signal molecules in *hospite*. Mar. Biol. **157**:1105–1111.
51. **Muscatine L, Porter JW.** 1977. Reef corals: mutualistic symbioses adapted to nutrient-poor environments. BioScience **27**:454–460.
52. **Wang J, Douglas A.** 1999. Essential amino acid synthesis and N recycling in an alga-invertebrate symbiosis. Mar. Biol. **135**:219–222.
53. **Allemand D, Tambutté E, Zoccola D, Tambutté S.** 2011. Coral calcification, cells to reefs, p 119–150. *In* Dubinsky Z, Stambler N (ed), Coral reefs: an ecosystem in transition. Springer Science, Dordrecht, Netherlands.